Chinese Journal of Natural Medicines

Si-Miao-Yong-An Decoction alleviates thromboangiitis obliterans by regulating miR-548j-5p/IL-17A signaling pathway

Chu CHU, Shangwen SUN, Zhen ZHANG, Qi WU, Haoyang LI, Gang LIANG, Xiuming MIAO, Haiqiang JIANG, Yan GAO, Yunhong ZHANG, Bin WANG, Xia LI

Citation: Chu CHU, Shangwen SUN, Zhen ZHANG, Qi WU, Haoyang LI, Gang LIANG, Xiuming MIAO, Haiqiang JIANG, Yan GAO, Yunhong ZHANG, Bin WANG, Xia LI, Si-Miao-Yong-An Decoction alleviates thromboangiitis obliterans by regulating miR-548j-5p/IL-17A signaling pathway, Chinese Journal of Natural Medicines, 2024, 22(6), 541-553. doi: 10.1016/S1875-5364(24)60626-6.

View online: https://doi.org/10.1016/S1875-5364(24)60626-6

Available online at www.sciencedirect.com

ScienceDirect

Chinese Journal of Natural Medicines 2024, **22**(6): 541-553
doi: 10.1016/S1875-5364(24)60626-6

Chinese Journal of Natural Medicines

•Original article•

Si-Miao-Yong-An Decoction alleviates thromboangiitis obliterans by regulating miR-548j-5p/IL-17A signaling pathway

CHU Chu[1Δ], SUN Shangwen[2, 3Δ], ZHANG Zhen[1Δ], WU Qi[4], LI Haoyang[5], LIANG Gang[4], MIAO Xiuming[4], JIANG Haiqiang[1], GAO Yan[6], ZHANG Yunhong[1], WANG Bin[4*], LI Xia[1*]

[1] *Innovative Institute of Chinese Medicine and Pharmacy, Shandong University of Traditional Chinese Medicine, Jinan 250355, China;*
[2] *National Key Laboratory for Innovation and Transformation of Luobing Theory; The Key Laboratory of Cardiovascular Remodeling and Function Research, Chinese Ministry of Education, Chinese National Health Commission and Chinese Academy of Medical Sciences; Department of Cardiology, Qilu Hospital of Shandong University, Jinan 250012, China;*
[3] *School of Clinical and Basic Medical Sciences, Shandong First Medical University & Shandong Academy of Medical Sciences, Jinan 271016, China;*
[4] *Affiliated Hospital of Shandong University of Traditional Chinese Medicine, Jinan 250014, China;*
[5] *International Business School, Tianjin Foreign Studies University, Tianjin 300204, China;*
[6] *Institute of Pharmaceutical Research, Shandong University of Traditional Chinese Medicine, Jinan 250355, China*

Available online 20 Jun., 2024

[ABSTRACT] Thromboangiitis obliterans (TAO) is a rare, chronic, progressive, and segmental inflammatory disease characterized by a high rate of amputation, significantly compromising the quality of life of patients. Si-Miao-Yong-An decoction (SMYA), a traditional prescription, exhibits anti-inflammatory, anti-thrombotic, and various other pharmacological properties. Clinically, it was fully proved to be effective for TAO therapy, but the specific therapeutic effect of SMYA on TAO has been unknown. Thus, deep unveiling the mechanism of SMYA in TAO for identifying clinical therapeutic targets is extremely important. In this study, we observed elevated levels of IL-17A in the peripheral blood mononuclear cells (PBMCs) of TAO patients, whereas the expression of miR-548j-5p was significantly decreased. A negative correlation between the levels of miR-548j-5p and IL-17A was also demonstrated. *In vitro* experiments showed that overexpression of miR-548j-5p led to a decrease in IL-17A levels, whereas downregulation of miR-548j-5p showed the opposite effect. Using a dual luciferase assay, we confirmed that miR-548j-5p directly targets IL-17A. Furthermore, serum containing SMYA effectively decreased IL-17A levels by increasing the expression of miR-548j-5p. More importantly, the results of *in vivo* tests indicated that SMYA mitigated the development of TAO by inhibiting IL-17A through the upregulation of miR-548j-5p in vascular tissues. In conclusion, SMYA significantly enhances the expression of miR-548j-5p, thereby reducing the levels of the target gene IL-17A and alleviating TAO. Our research not only identifies novel targets and pathways for the clinical diagnosis and treatment of TAO but also advances the innovation in traditional Chinese medicine through the elucidation of the SMYA/miR-548j-5p/IL-17A regulatory axis in the pathogenesis of TAO.

[KEY WORDS] Thromboangiitis obliterans; IL-17A; Inflammation; miR-548j-5p; Si-Miao-Yong-An Decoction

[CLC Number] R965 **[Document code]** A **[Article ID]** 2095-6975(2024)06-0541-13

[Received on] 23-Oct.-2023

[Research funding] This work was supported by the Natural Science Foundation of China (No. 82274575), Co-construction Project of State Administration of TCM (Nos. GZY-KJS-SD-2023-034, GZY-KJS-SD-2023-046), Major Basic Research Project of Natural Science Foundation of Shandong Province (No. ZR2023ZD56), the Joint Fund of Natural Science Foundation of Shandong (No. ZR2022LZY011), the Central Government Guides Local Science and Technology Development Fund Projects of Shandong Province (No. YDZX20203700001407), Taishan Scholars (No. Tsqn201812125), National Youth Qihuang Scholar Training Program, Shandong Province Traditional Chinese Medicine High Level Talent Cultivation Project and Key research and development project of Shandong Province (No. 2020CXGC010505).

[*Corresponding author] E-mails: 71000848@sdutcm.edu.cn (WANG Bin); 60230033@sdutcm.edu.cn (LI Xia)

[Δ]These authors contributed equally to this work.

These authors have no conflict of interest to declare.

Introduction

Thromboangiitis obliterans (TAO) is a segmental, inflammatory, and thrombo-occlusive disease affecting the peripheral vascular system, particularly the small arteries and veins of the upper and lower extremities. Predominantly observed in the Middle East, Far East, Southeast Asia, Eastern Europe, and South America, TAO typically manifests between the ages of 20 and 50, with male smokers being the most vulnerable demographic [1, 2]. The initial clinical symptoms are ischemic in nature, resulting from the stenosis or occlusion of distal arterioles and veins. Disease progression leads to severe symptoms, including calf intermittent claudication, rest pain, and ischemic ulcerations, which may ultimately result in amputation or death. Prospective studies have shown that 34% of patients with TAO undergo amputa-

tion within 15 years of diagnosis, and the average age at death is 52 years [3]. Given these dire outcomes, the prevention and treatment of TAO are of paramount importance. However, the effective management of TAO is currently challenged by a significant gap in our understanding of its pathogenesis, which impedes early diagnosis and effective therapeutic interventions.

Si-Miao-Yong-An Decoction (SMYA), a traditional Chinese medicine formula, is composed of *Lonicera japonica* Thunb (Jinyinhua, Flower), *Scrophularia ningpoensis* Hemsl (Xuanshen, Root), *Angelica sinensis* (Oliv.) Diels (Danggui, Root), and *Glycyrrhiza uralensis* Fisch (Gancao, Stem) with a weight ratio of 3 : 3 : 2 : 1 [4]. This formula first appeared in the "*Hua Tuo Shen Yi Mi Zhuan*" during the Eastern Han Dynasty and was later included in the "*Yan Fang Xin Bian*" of the Qing Dynasty [5]. Historically used to treat gangrene, SMYA is currently employed in modern medicine primarily for the treatment of peripheral vascular diseases. Its efficacy is attributed to its properties of clearing heat, detoxifying, activating blood circulation, unblocking collaterals, and relieving pain. Furthermore, SMYA has been proven to possess anti-inflammatory, lipid-lowering, plaque-stabilizing, and anti-thrombotic pharmacological effects [6-9]. Although long-term clinical practice has confirmed SMYA's beneficial effects on TAO [10], the mechanisms behind its therapeutic impact remain unclear. Elucidating these mechanisms is crucial for guiding molecular diagnosis and developing targeted therapies for TAO.

MicroRNAs (miRNAs) are endogenous, small, non-coding, single-stranded RNAs comprising 22 to 24 nucleotides. They function by downregulating the expression of target genes, specifically by binding with incomplete complementary [11, 12] to the 3' untranslated regions (3'UTRs) of these genes. MiRNAs are integral to various cellular processes, including those occurring in monocytes, macrophages, and endothelial cells [13-17]. Additionally, they play a critical role in the development and progression of various vascular diseases, such as coronary atherosclerotic heart disease, cerebral infarction, arteriosclerosis obliterans, and deep vein thrombosis [18-20]. Notably, miRNAs also influence the formation and progression of TAO by modulating inflammation [21, 22]. Given their significant roles, the investigation of novel miRNAs with potential therapeutic effects on TAO is a promising area of research.

Inflammation is a key contributor to endothelial damage and dysfunction, which are significant risk factors for TAO [23-25]. Interleukin-17A (IL-17A), a pro-inflammatory cytokine with wide-ranging effects, is implicated in the pathogenesis of various arterial diseases. It does so by orchestrating the release of cytokines and inflammatory molecules from a variety of cells, including epithelial cells, endothelial cells, and fibroblasts [26-28]. Furthermore, elevated levels of IL-17A are known to increase coagulation factors and activate platelets, leading to thrombosis [29, 30]. Despite these insights, the specific role of IL-17A-mediated inflammatory processes in the progression of TAO remains to be elucidated.

In this study, we observed an elevation in IL-17A expression in the peripheral blood mononuclear cells (PBMCs) of patients with TAO. Conversely, miR-548j-5p was found to be downregulated in these patients, as determined by miRNA microarray analysis. Our findings indicate that miR-548j-5p can decrease IL-17A levels by targeting its 3'UTR, thereby contributing to the improvement of TAO symptoms. Furthermore, we explored the functions and mechanisms of SMYA in alleviating TAO. The results demonstrated that SMYA prevents TAO by promoting the expression of miR-548j-5p, which subsequently downregulates IL-17A. Collectively, our data suggest that the therapeutic effects of SMYA on TAO are mediated through the reduction of IL-17A *via* the enhancement of miR-548j-5p expression. This novel insight presents a promising intervention strategy for TAO.

Materials and Methods

Preparation of SMYA

The herbal constituents for SMYA were procured from the First Affiliated Hospital of Shandong University of Traditional Chinese Medicine. The ingredients — *Lonicera japonica* Thunb, *Scrophularia ningpoensis* Hemsl, *Angelica sinensis* (Oliv.) Diels, and *Glycyrrhiza uralensis* Fisch —were carefully weighed in a ratio of 3 : 3 : 2 : 1. All herbs were combined and decocted in distilled water at a 1 : 8 weight/volume ratio. The mixture was heated to 100 ℃ for a total of 60 min, divided into two sessions: 40 min initially, followed by a second session of 20 mins, with the process being repeated once more. Following the second decoction, the two extracts were combined and filtered. The resulting solution was then concentrated to a final volume using a freeze dryer (Posen Instrument Co., Ltd., Jinan, China), resulting in 66 g of dried powdered extract. This powder was stored at −80 ℃ and dissolved in double-distilled water (ddH2O) for subsequent use.

Liquid chromatography (LC) mass spectrometry (MS)/MS analysis

The LC-MS and MS/MS data were analyzed using a UHPLC Ultimate 3000 instrument coupled with a Q-Exactive Orbitrap-MS spectrometer (Thermo Fisher Scientific, CA, USA), employing a method similar to that previously described [31]. The chromatographic gradient was set as follows: from 0 to 2 min, 2% solvent B; from 2 to 30 min, a gradient increase from 2% to 52% solvent B; from 30 to 32 min, an increase from 52% to 90% solvent B; and from 32 to 32.2 min, a sharp decrease from 90% back to 2% solvent B.

Patients

This study included 20 patients diagnosed with thromboangiitis obliterans (TAO) (recruited from October 2020 to January 2022) and 20 healthy control subjects from the Affiliated Hospital of Shandong University of Traditional Chinese Medicine (Table 1).

The inclusion criteria for TAO patients were aligned with Shionoya's criteria: 1) age < 50 years at onset, 2) a his-

Table 1 Baseline characteristics of TAO patients and healthy controls.

Characteristics	TAO (n = 20)	Control (n = 20)
Age, years (mean ± SD)	40.7 ± 9.6	42.2 ± 8.9
Gender, females/males	1/19	3/17
Weight (kg, mean ± SD)	60.2 ± 12.4	62.3 ± 15.6
BMI ($kg \cdot m^{-2}$, mean ± SD)	24.2 ± 6.4	26.1 ± 6.6
Recent immobilization/Surgery	0	0
Anti-coagulants or platelet-inhibitors	0	0
Hormone	0	0
Smoking	14	5
Hypertension	0	0
Diabetes mellitus	0	0
Other chronic diseases	0	0

tory of smoking, 3) infrapopliteal arterial occlusion, 4) involvement of either the upper limbs or presence of phlebitis migrans, 5) absence of atherosclerotic risk factors other than smoking, and 6) confirmation *via* Doppler ultrasound. Exclusion criteria were set as follows: patients with peripheral arterial diseases or immune abnormalities attributable to causes other than TAO [32].

Specimen collection

Intravenous blood samples were collected after overnight fasting, and serum was isolated within 2 h of collection. PBMCs were isolated using Ficoll density gradient centrifugation and a human peripheral blood lymphocyte separation solution (Solarbio, Beijing, China).

Microarray analysis

Total RNA was extracted from PBMCs of 3 TAO patients and 3 control subjects and analyzed using miRNA microarray technology by OE Biotechnology Company (Shanghai, China). Differentially expressed miRNAs were selected based on a significance threshold of $P < 0.05$ for further research.

Quantitative Real-Time PCR (qRT-PCR)

Total RNA was extracted from PBMCs using the TRIzol reagent (Invitrogen, Carlsbad, CA) following the manufacturer's instruction. RNA was reversed transcribed with miRNA first strand cDNA synthesis Kit (Vazyme, Nanjing, China) or the Prime Script RT Reagent Kit (Toyobo, Osaka, Japan) for mRNA according to the manufacturer's instructions.

Quantitative real-time polymerase chain reaction (qRT-PCR) was conducted using SYBR Green (Invitrogen) on an Applied Biosystems QuantStudio 1 Plus instrument (Thermo Fisher Scientific). GAPDH and U6 served as reference genes for normalizing the expression levels of mRNA and miRNA, respectively. Primer sequences used for the PCR are listed in Table 2. Each sample was amplified in triplicate. Relative quantification of RNA was performed using the comparative $2^{-\Delta\Delta Ct}$ method.

Enzyme-Linked Immunosorbent Assay (ELISA)

Human serum and supernatant from Human Umbilical Vein Endothelial Cells (HUVECs) were analyzed for IL-17A using a hypersensitivity kit designed for human samples, while rat vascular tissues were examined using a rat-specific IL-17A ELISA kit (Multi Sciences, Hangzhou, China), following the manufacturers' instructions. Optical density (OD) readings at dual wavelengths (450 nm and 630 nm) were obtained using a microplate reader. These readings were used to construct a standard curve based on the OD values of the provided standards, enabling the quantification of IL-17A protein levels.

Western blotting assay

Total protein was extracted using RIPA reagent (Solarbio, Beijing). A 10 μg sample of each protein was subjected to electrophoresis on either 8% or 12% SDS-PAGE and subsequently transferred to a nitrocellulose membrane. The membrane was blocked with 5% skim milk at room temperature for 1 h. It was then incubated overnight at 4 °C with the following primary antibodies: anti-rat eNOS (1 : 500, ab300071, Abcam, UK), anti-rabbit vWF (1 : 1000, ab174290, Abcam, UK), anti-rabbit GAPDH (1 : 10 000, ab181603, Abcam, UK), and anti-rabbit TF (1 : 1000, A1378, ABclonal, China). After washing, the membrane was incubated with HRP-conjugated secondary antibodies on a shaking table at room temperature. Detection was carried out using Immobilon Western Chemiluminescent HRP Substrate (Millipore, WBKLS0500), and the blots were scanned using a Bio-Rad gel imaging system.

Dual-luciferase reporter assay

Fragments of the 3'UTR from human IL-17A mRNA (both wild-type and mutant) were amplified and cloned into the pGL3-3M Luc vector (Promega, Madison, WI, USA) to generate luciferase reporter vectors for the wild-type (WT) and mutant (MUT) human IL-17A mRNA 3'UTR, respectively. 293T cells were transfected with the luciferase reporter plasmids and either miR-548j-5p mimics or negative control (NC) at a final concentration of 100 $nmol \cdot L^{-1}$. After 24 h post-transfection, the cells were collected, and the ratio of firefly to renilla luciferase luminescence was measured using the Dual-Luciferase Reporter Assay System (Promega, Madison) on a GloMax 20/20 photometer (Promega, Madison).

Network pharmacological analysis of SMYA

To integrate and analyze data on SMYA's treatment of TAO, we screened for effective components and their associ-

Table 2 Real-time quantitative PCR (qRT-PCR) primers used in this study.

Gene	Sequences (5'-3')
GAPDH (Homo sapiens)	F: GCACCGTCAAGGCTGAGAAC
	R: TGGTGAAGACGCCAGTGGA
Actin (Rattus norvegicus)	F: CTCTGTGTGGATTGGTGGCT
	R: CGCAGCTCAGTAACAGTCCG
IL-17A (Homo sapiens)	F: ATTGGTGTCACTGCTACTGCT
	R: AGGTTGACCATCACAGTCCG
IL-17A (Rattus norvegicus)	F: ATCCATGTGCCTGATGCTGTT
	R: AAGTTATTGGCCTCGGCGTT

ated targets within the Traditional Chinese Medicine System Pharmacology (TCMSP) database. The action targets of the active ingredients were subsequently identified in the TCMSP database, and their names were standardized using the UniProt database. We then searched for relevant TAO targets in the Comparative Toxicogenomics (CTD) database using "thromboangiitis obliterans" as the keyword. Using the online tool Venny diagram analysis, we identified the target genes of SMYA for treating TAO. Additionally, pathway enrichment analysis was conducted using the Kyoto Encyclopedia of Genes and Genomes (KEGG) pathways in the Metascape database, from which a bubble map was generated to visually represent the findings.

TAO rat model and treatment

Eight-week-old male Wistar rats weighing 200 g were obtained from Beijing Huafukang Biotechnology Co., Ltd. (Beijing, China). The animal experiments were conducted in accordance with the Guide for the Protection and Utilization of Experimental Animals (Shandong University of Traditional Chinese Medicine) and were approved by the Animal Protection and Utilization Committee of Shandong University of Traditional Chinese Medicine. Vasculitis in the left hind limb of rats was induced using sodium laurate, as described in previous studies [22].

The rats were randomly assigned to six groups (5 rats per group): a Control group (no surgical intervention), a Sham operation group, a TAO Control group, and TAO groups treated with high, middle, and low doses of SMYA. Using the equivalent dose ratio based on body surface area conversion between humans and animals, the dose conversion factor was 6.3 between rats and humans. For this study, the standard dose of SMYA was set at 28 g (crude drug) per kg per day (composition ratio = 3 : 3 : 2 : 1) [33]. Accordingly, SMYA was administered by gavage at 14 $g \cdot kg^{-1} \cdot d^{-1}$ in the low-dose group, 28 $g \cdot kg^{-1} \cdot d^{-1}$ in the middle-dose group, and 56 $g \cdot kg^{-1} \cdot d^{-1}$ in the high-dose group. The Control and Sham TAO groups received an equivalent volume of distilled water. After seven days of continuous intragastric administration, vascular Doppler ultrasounds were performed 2 h after the last dose [34]. Subsequently, the animals were euthanized, and thrombi or vascular tissues were collected and fixed [35] in 4% paraformaldehyde for H&E staining, qRT-PCR, and Western blotting analyses.

For miR-548j-5p rescue experiments, rats were further divided into TAO Control, TAO SMYA, TAO SMYA + INC, and TAO SMYA + miR-548j-5p inhibitor groups (5 per group). Each rat in the TAO model was intragastrically administered high-dose SMYA or distilled water for seven days. On the last day of administration, miR-548j-5p inhibitor or INC (45 nmol diluted in 200 μL PBS) was injected into the rat tail vein in the respective groups. The rats in the TAO SMYA group received the same volume of PBS. Vascular tissues were collected 2 h post-injection.

For the IL-17A inhibitor administration experiments, the rats were divided into TAO + anti-IL-17A and TAO + NS groups (n = 5 per group). Rats in the anti-IL-17A group were treated with an anti-IL-17A antibody (0.1 $mg \cdot kg^{-1}$ body weight intravenously for five days) (Clone: 17F3, eBioscience, Frankfurt, Germany) [36]. The TAO + NS group received an equivalent amount of normal saline. Two hours after the final injection, the rats were euthanized, and the thrombi were collected.

Preparation of medicated serum

Wistar rats were randomly divided into two groups (n = 5 each): (1) blank group and (2) medication administration groups (receiving 14, 28, and 56 $g \cdot kg^{-1} \cdot d^{-1}$). Rats in the medication groups received their respective doses once daily for seven consecutive days, while the blank group was administered an equivalent volume of distilled water daily for the same period. Two hours after the last dose, blood was collected *via* retroorbital bleeding, allowed to stand for 1 h, and then centrifuged at 3000 $r \cdot min^{-1}$ for 10 min to separate the serum. The serum was subsequently inactivated in a water bath at 56 °C for 30 min and filtered through a 0.22 μm sterile microporous membrane. It was then stored at −80 °C for future use.

Cell lines, culture conditions, and cell transfection

293T cells and HUVECs were obtained from the BeNa Culture Collection (Beijing, China). Both cell types were cultured in DMEM or DMEM F12 nutrient medium (Bioind, Kibbuiz, Israel) supplemented with 10% fetal bovine serum (FBS) and 1% penicillin/streptomycin. The cells were maintained in a humidified atmosphere containing 5% CO2 at 37 °C.

To investigate the regulatory effects of miR-548j-5p on IL-17A, miR-548j-5p mimics, NC, miR-548j-5p inhibitor, and inhibitor NC (INC) (GenePharma, Shanghai, China) were transfected into HUVECs at a concentration of 100 $nmol \cdot L^{-1}$ using Lipofectamine™ 2000 (Invitrogen, Carlsbad, USA). The cells were incubated under the same conditions for 24 h post-transfection. The sequences of the mimics and inhibitors used for miR-548j-5p overexpression and inhibition are detailed in Table 3.

To examine the effects of SMYA-containing serum on endothelial cells, HUVECs were co-cultured with blank serum or SMYA-containing serum from the Low (10% of 14 $g \cdot kg^{-1} \cdot d^{-1}$), Middle (10% of 28 $g \cdot kg^{-1} \cdot d^{-1}$), and High (10% of 56 $g \cdot kg^{-1} \cdot d^{-1}$) groups for 24 h at 37 °C and 5% CO2. In a miR-548j-5p rescue experiment conducted *in vitro*, HUVECs were co-cultured with 56 $g \cdot kg^{-1} \cdot d^{-1}$ SMYA-containing serum for 24 h, followed by transfection with either INC or miR-548j-5p inhibitor at the previously mentioned concentration. Subsequent experiments were performed after an additional 24-h incubation.

Rat Doppler ultrasound

Images of the surrounding structures and blood vessels were obtained using the VINNO6 LAB system [37].

Hematoxylin and Eosin (H&E)

The experimental methods followed those described in our previous work [20]. Tissue sections were mounted with

Table 3 The sequences of synthesized mimic, negative control (NC), inhibitor, and inhibitor NC.

Gene	Sequences (5'-3')
hsa-miR-548j-5p mimics	AAAAGUAAUUGCGGUCUUUGGU
	CAAAGACCGCAAUUACUUUUUU
NC	UUCUCCGAACGUGUCACGUTT
	ACGUGACACGUUCGGAGAATT
hsa-miR-548j-5p inhibitor	ACCAAAGACCGCAAUUACUUUU
Inhibitor NC	CAGUACUUUUGUGUAGUACAA

neutral resin and examined under a light microscope (IX73, Olympus, Japan) for pathological analysis.

Statistical analyses

Unless otherwise specified, all experiments were independently repeated at least three times. Data are expressed as the mean ± SD. Statistical comparisons between two groups were conducted using a two-tailed unpaired Student's *t*-test after ensuring normality and equal variance with appropriate tests. For analyses involving multiple comparisons, a one-way analysis of variance (ANOVA) followed by a Bonferroni post hoc test was used. Data visualization was performed using GraphPad Prism version 9.5. Statistical analyses were conducted using SPSS version 19.0. Pearson correlation analysis was utilized to assess correlations, and the receiver operating characteristic (ROC) curve was used to evaluate diagnostic value. A *P*-value of less than 0.05 was considered statistically significant.

Results

SMYA promoted artery thrombi resolve in vivo

SMYA is a traditional prescription used in the treatment of thromboangiitis TAO. To further elucidate the therapeutic role of SMYA in TAO, we administered various doses of SMYA to a TAO rat model. Both H&E staining and Doppler ultrasound assessments demonstrated a dose-dependent reduction in the thrombus area in the Low-dose, Middle-dose, and High-dose SMYA-treated rat groups (Figs. 1A–1C). Additional data on H&E staining for the normal control and sham groups can be found in the supplementary material. Furthermore, the length and weight of the thrombi decreased with increasing doses of SMYA (Figs. 1D–1E). Collectively, these results suggest that SMYA effectively reduces the formation of thrombi in TAO.

SMYA-containing serum downregulates IL-17A mRNA and protein expressions in vitro

To investigate the chemical composition of SMYA, we employed LC-MS/MS analysis in both positive and negative ion modes, identifying several chemical substances, including luteolin, z-p-luteolin, and glycinol dispersant (Figs. 2A–2B). The detailed results of the LC-MS/MS analysis are provided in table s1. To explore the mechanism behind SMYA's therapeutic activity on TAO, network pharmaco-

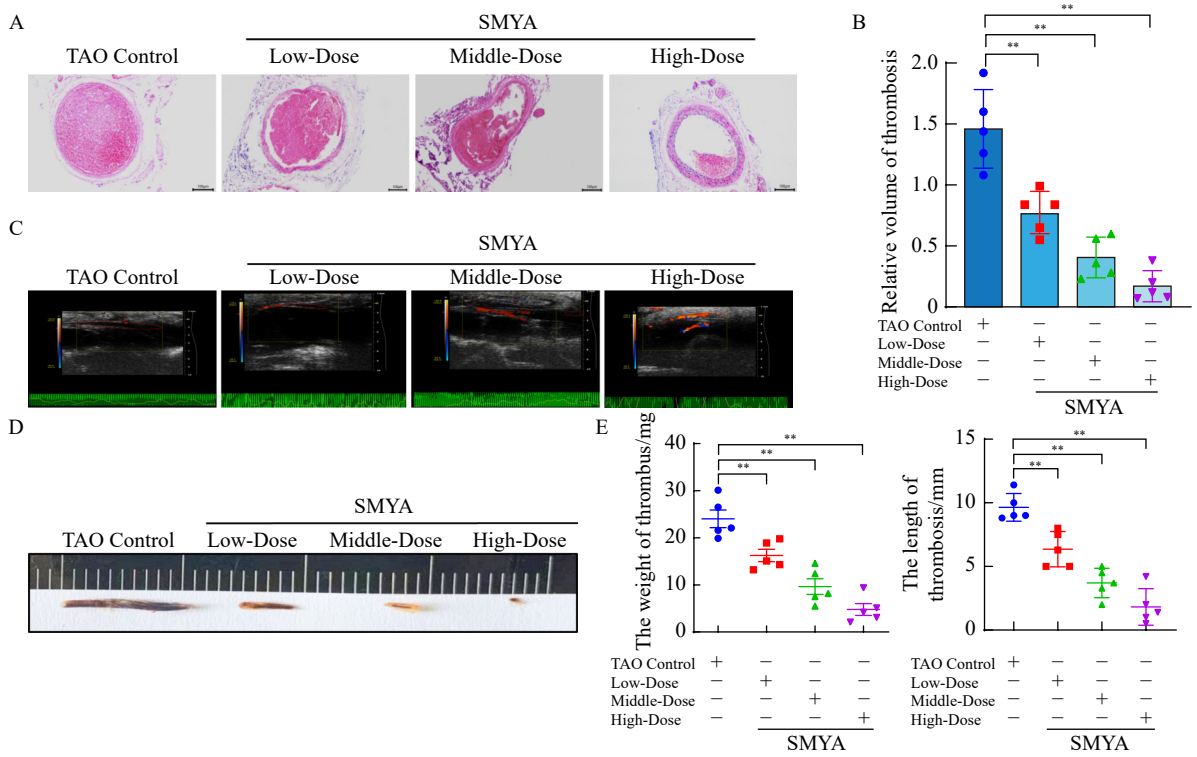

Fig. 1 SMYA promoted artery thrombi resolve *in vivo*. (A, B) H&E staining (magnification, × 100), scale bars = 100 μm analysis of rat vessel transverse section from TAO Control, Low, Middle, and High (SMYA decoction) at seven days (n = 5). (C) Doppler ultrasound analysis of rat vessels from TAO Control, Low, Middle, and High (SMYA decoction) at seven days (n = 5). (D, E) The changes of thrombus size and volume after being infused with TAO Control, Low, Middle and High concentration SMYA decoction for seven days (n = 5). Data are presented as the mean ± SD (n = 5). $^{**}P < 0.01$ *vs* TAO Control.

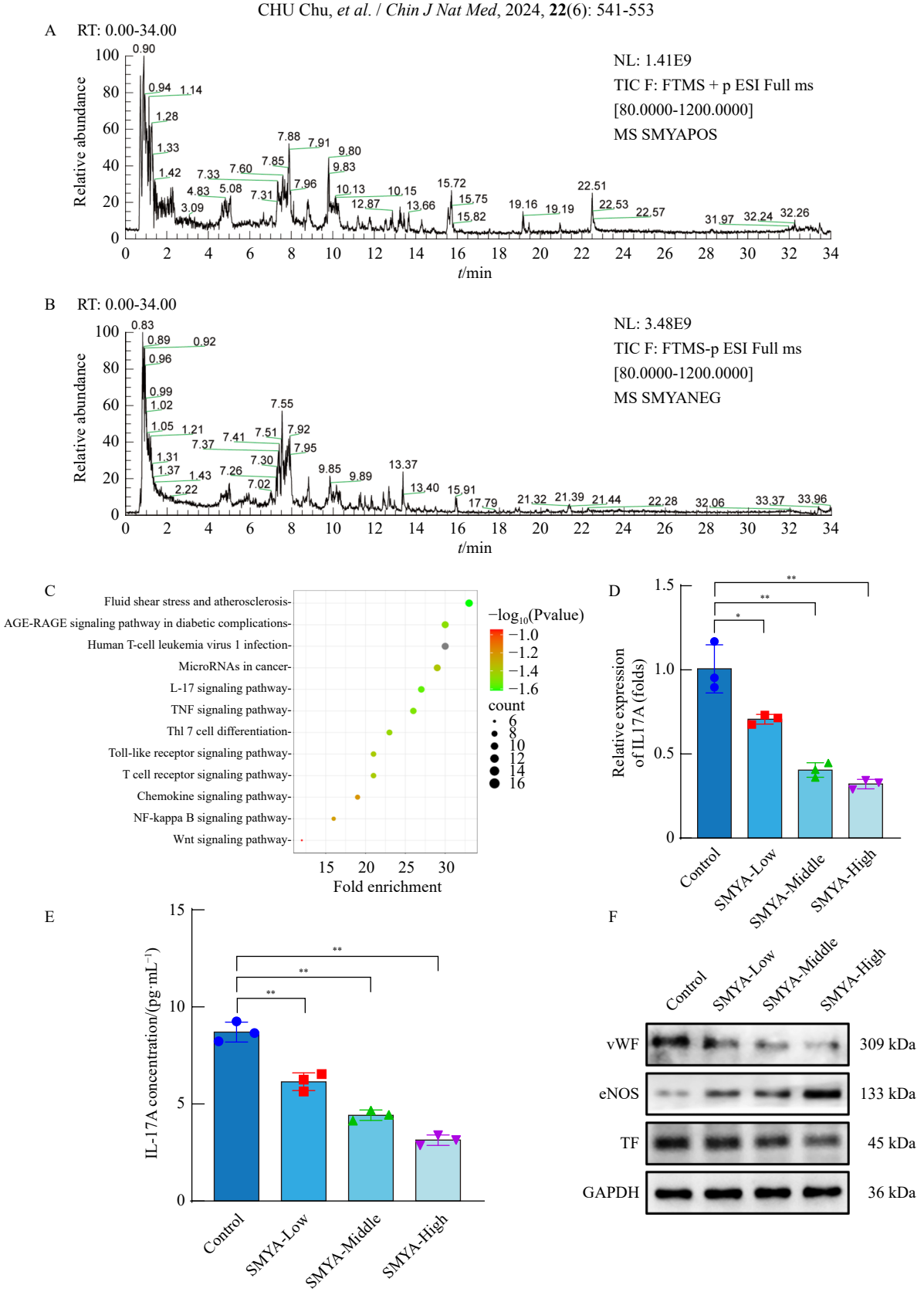

Fig. 2 SMYA-containing serum downregulated *IL-17A* mRNA and protein expression *in vitro*. (A, B) LC-MS/MS spectrums of SMYA under positive ion and negative ion mode. (C) The active components of SMYA act on the signal pathway of TAO. (D, E) *IL17A* mRNA and protein levels were respectively analyzed utilizing qRT-PCR and ELISA in HUVECs of Control, SMYA-Low group, SMYA-Middle group, and SMYA-High group. (F) Detection of VWF, eNOS, and TF protein expressions using Western blotting in HUVECs of Control, SMYA-Low group, SMYA-Middle group, and SMYA-High group. Data are presented as the mean ± SD. $^{*}P < 0.05$, $^{**}P < 0.01$ *vs* Control.

logy was utilized to identify 201 key targets of SMYA relevant to TAO. Following the screening criteria, KEGG pathway enrichment analysis revealed 208 significant pathways ($P < 0.01$), such as the IL-17 signaling pathway, miRNAs in cancer signaling pathway, and toll-like receptor signaling pathway (Fig. 2C). Subsequently, HUVECs were co-cultured with either control serum or SMYA-containing serum at varying concentrations (10% of 14 $g \cdot kg^{-1} \cdot d^{-1}$, 28 $g \cdot kg^{-1} \cdot d^{-1}$, and 56 $g \cdot kg^{-1} \cdot d^{-1}$) for 24 h. We observed that the expression of IL-17A mRNA and protein was inversely correlated with the concentration of the drug-containing serum (Figs. 2D–2E). Additionally, the expression of vWF and TF proteins in HUVECs exhibited a dose-dependent decrease, while eNOS protein expression increased in a gradient manner (Fig. 2F). These findings suggest that SMYA may attenuate IL-17A expression through the regulation of miR-548j-5p, thereby impacting vascular function. Collectively, our results indicate that SMYA effectively reduces IL-17A mRNA and protein expression, influencing the normal function of the vasculature.

Dysregulation of IL-17A is involved in the formation of TAO

To explore the involvement of IL-17A in the progression of TAO, we initiated our investigation by conducting qRT-PCR and ELISA analyses. These tests revealed a significant increase in IL-17A mRNA and protein levels in the PBMCs and serum of TAO patients compared to controls (Figs. 3A–3B). To further assess the role of IL-17A *in vivo*, we developed TAO rat models. H&E staining and Doppler ultrasound examinations indicated that 100% (5 out of 5) of the TAO models developed thrombosis, whereas the normal control group and sham operation group exhibited no thrombus formation (Figs. 3C–3D). In comparison to the normal control and sham operation rats, the vascular tissue of TAO rats showed significantly increased protein expression of tissue factor (TF) and von Willebrand factor (vWF), along with a significant decrease in endothelial nitric oxide synthase (eNOS) protein levels (Fig. 3E). Moreover, both IL-17A mRNA in PBMCs and protein levels in the vascular tissue of TAO rats were significantly elevated compared to those in the normal control and sham group rats (Figs. 3F–3G). To determine the pathogenic role of IL-17A in TAO, we administered an anti-IL-17A antibody to neutralize IL-17A activity in the rats. Subsequent H&E staining of the thrombus areas in control and anti-IL-17A-treated rats demonstrated a significant reduction in thrombus size seven days post-treatment (Fig. 3H).

miR-548j-5p is downregulated in TAO patients and negatively correlated with IL-17A

To identify miRNAs responsible for regulating IL-17A expression, we conducted a miRNA microarray analysis, re-

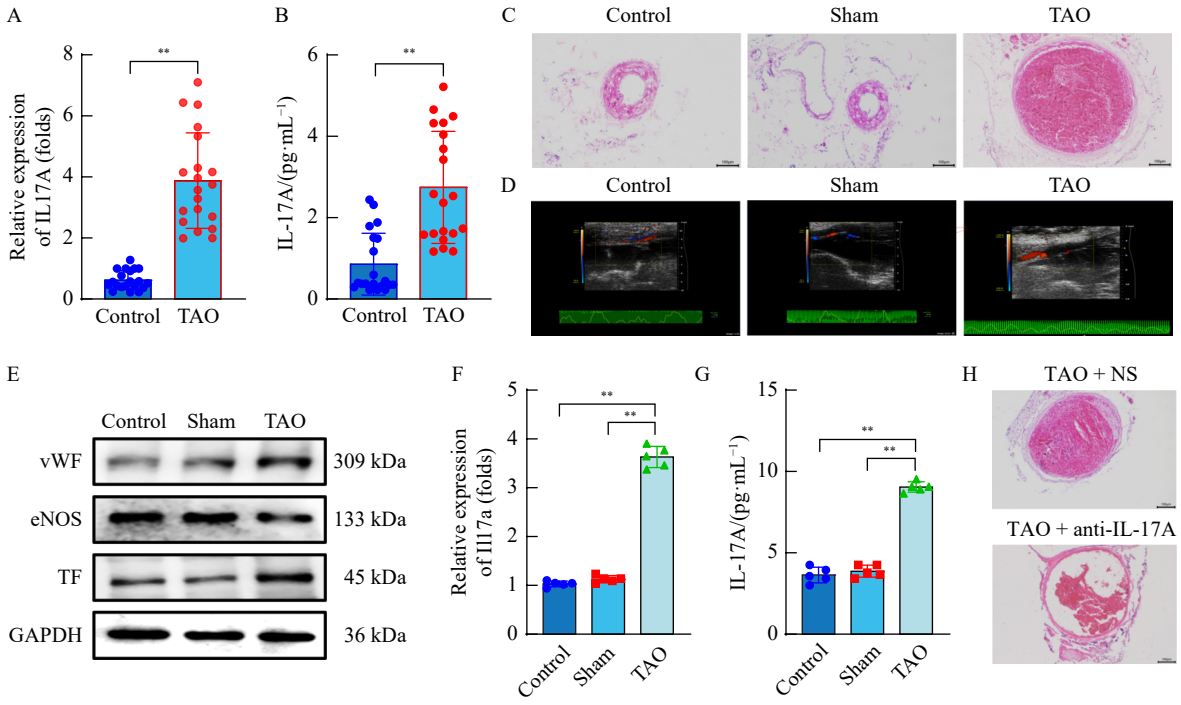

Fig. 3 Dysregulation of IL-17A is involved in the formation of TAO. (A) Measurement of *IL17A* mRNA expressions in PBMCs from TAO patients and healthy people by qRT-PCR ($n = 20$). (B) IL-17A protein levels were determined in the serum of TAO patients and healthy people by ELISA. ($n = 20$). (C, D) H&E staining (magnification, × 100), scale bar = 100 μm and Doppler ultrasound of thrombus from Control, Sham, and TAO groups ($n = 5$). (E) Protein levels of vWF, eNOS and TF were tested by Western blotting in the vascular tissue of rats in the Control, Sham, TAO groups ($n = 5$). (F, G) IL-17A mRNA and protein expressions were respectively measured by qRT-PCR and ELISA in the vascular tissue of rats in the Control, Sham, and TAO groups ($n = 5$). (H) H&E staining (magnification, × 100) of thrombus from the Control group and neutralizing antibody group ($n = 5$), scale bars = 100 μm. Data are presented as the mean ± SD ($n = 5$), $^{**}P < 0.01$ *vs* Control.

vealing 41 miRNAs that were downregulated in TAO patients compared to healthy controls. Considering the association of TAO with IL-17A, we utilized Chip, TargetScan, and miRDB to identify potential miRNAs that negatively regulate IL-17A at transcriptional and post-transcriptional levels (Fig. 4A). qRT-PCR analysis indicated that miR-548j-5p levels were significantly downregulated in TAO patients relative to healthy controls (Fig. 4B). Additionally, a statistically significant negative correlation ($P = 0.0087$, $r = -0.5698$) was observed between miR-548j-5p and IL-17A expression (Fig. 4C), implicating miR-548j-5p in TAO. ROC analysis demonstrated that miR-548j-5p expression in PBMCs could accurately distinguish TAO patients from healthy donors, with an area under the curve (AUC) of 0.9075 (95% confidence interval: 0.8146 to 1.000) (Fig. 4D). These findings suggest that reduced miR-548j-5p may elevate IL-17A expression in TAO, establishing a functional relationship between miR-548j-5p and IL-17A in the disease's formation and progression.

To further explore the regulatory effect of miR-548j-5p on IL-17A, we manipulated its expression in HUVECs using specific mimics and inhibitors. The results revealed that transfection with miR-548j-5p mimics increased miR-548j-5p levels and subsequently reduced IL-17A expression at both mRNA and protein levels, whereas the miR-548j-5p inhibitor produced opposite effects (Figs. 4E–4G). Compared to the negative control transfected HUVECs, the expression of TF and vWF decreased, while eNOS increased in the miR-548j-5p mimics group. Conversely, the opposite effects were observed when the miR-548j-5p inhibitor was used (Fig. 4H). The results suggested that miR-548j-5p might affect endothelial function by regulating IL-17A.

miR-548j-5p directly targets IL17A mRNA 3′UTR.

To elucidate the targeted regulatory relationship between miR-548j-5p and IL17A, a luciferase reporter assay was conducted. We co-transfected miR-548j-5p mimics and plasmids encodingboththewild-typeandmutant3′UTRofIL17A(Fig.5A). The miR-548j-5p mimics significantly inhibited the luciferase activity associated with the wild-type IL17A mRNA 3′UTR. In contrast, this suppressive effect was not observed with the mutant IL17A mRNA 3′UTR (Fig. 5B), indicating that IL17A is a direct target of miR-548j-5p.

miR-548j-5p inhibition attenuates the efficacy of SMYA-containing serum in vitro

To determine whether SMYA-containing serum mediates its effects through miR-548j-5p *in vitro,* HUVECs were co-cultured with SMYA-containing serum and then transfected with either INC (inhibitor negative control) or a miR-548j-5p inhibitor. qRT-PCR analysis showed that miR-548j-5p expression was detectable in HUVECs cultured with SMYA-containing serum (Fig. 6A). Subsequently, we transfected HUVECs cultured with high-dose serum with a miR-548j-5p inhibitor to suppress miR-548j-5p expression. The levels of miR-548j-5p in the inhibitor group were significantly lower

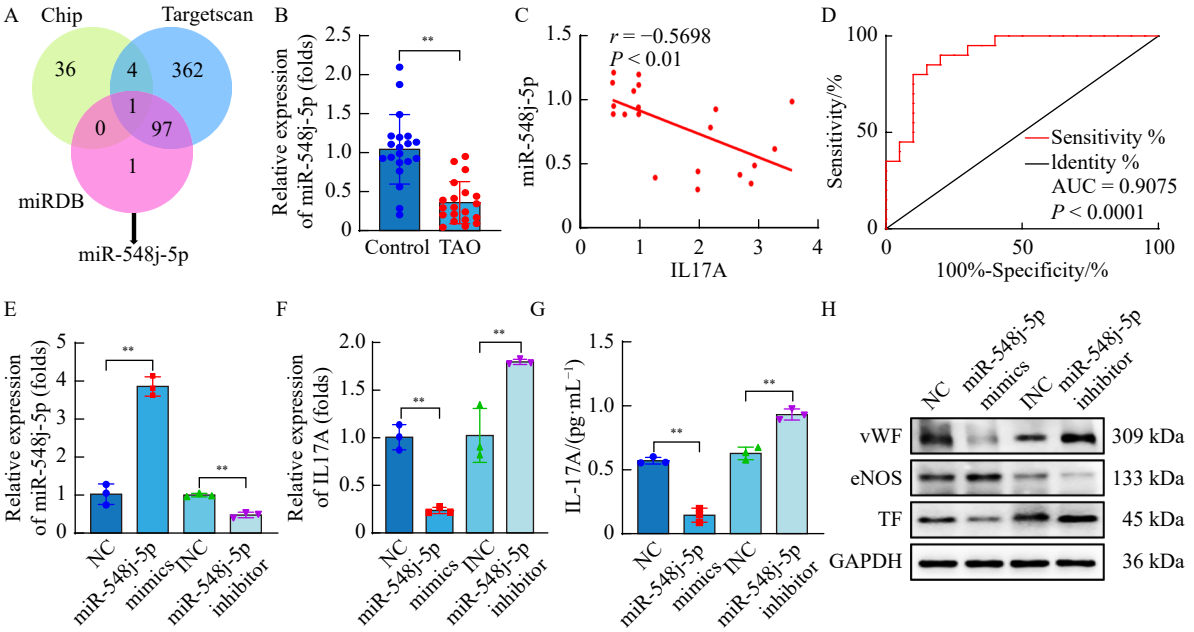

Fig. 4 miR-548j-5p is downregulated in TAO patients and negatively correlated with IL-17A. (A) Venn diagram of predictive miRNAs between Chip, TargetScan, and miRDB. (B) The significant downregulation of miR-548j-5p in TAO patients' PBMCs compared with that in healthy people using qRT-PCR ($n = 20$). (C) A distinctly negative correlation between miR-548j-5p and *IL17A* by Pearson correction analysis ($n = 20$). (D) ROC curve estimated the favoring diagnostic value of miR-548j-5p for TAO. (E, F) Experiments of qRT-PCR for detecting the expressions of miR-548j-5p and *IL17A* mRNA after NC, miR-548j-5p mimics, INC, and miR-548j-5p inhibitor transfection in HUVECs. (G) ELISA assays IL-17A protein level in HUVECs. (H) Protein expressions of vWF, eNOS, and TF in HUVECs were assessed by Western blotting. Data are presented as the mean ± SD ($n = 20$). $^{**}P < 0.01$ *vs* Control; $^{**}P < 0.01$ *vs* NC.

than in the INC group (Fig. 6B), and as a result, IL17A mRNA and protein expression increased (Figs. 6C–6D). Furthermore, the suppression of vWF and TF, along with the promotion of eNOS, were significantly mitigated (Fig. 6E). These results showed that SMYA regulates IL-17A through miR-548j-5p, thus affecting the normal function of vascular.

Inhibition of miR-548j-5p invalidates SMYA's therapeutic effect in vivo

To further explore whether SMYA exerts its therapeutic effects through miR-548j-5p *in vivo*, we administered either INC or a miR-548j-5p inhibitor via the tail vein following seven days of SMYA treatment in TAO rats. qRT-PCR analysis revealed that miR-548j-5p levels in the vascular tissue of TAO rats were significantly lower than those in the normal control and sham group rats(Fig. 7A). Following treatment, miR-548j-5p expression in the vascular tissues of rats treated with high-dose, middle-dose, and low-dose SMYA showed a gradient increase compared to the TAO group (Fig. 7B). Concurrently, the expression of IL-17A mRNA and protein demonstrated a gradient decrease (Figs. 7C–7D). Moreover, Western blotting analysis indicated that compared to the TAO group, the expressions of vWF and TF proteins in the vascular tissue of the SMYA-treated groups decreased gradually, while the expression of eNOS protein increased (Fig. 7E).

H&E staining demonstrated a significant increase in the thrombus area for the group that received the miR-548j-5p inhibitor injection compared with the high-dose SMYA + INC (inhibitor negative control) group (Fig. 7F). Further analysis revealed that, compared to the INC group, miR-548j-5p levels were reduced in the vascular tissue of TAO rats treated with the miR-548j-5p inhibitor (Fig. 7G). Correspondingly, IL-17A mRNA levels were significantly increased (Fig. 7H), along with enhanced IL-17A protein levels (Fig. 7I). Concur-

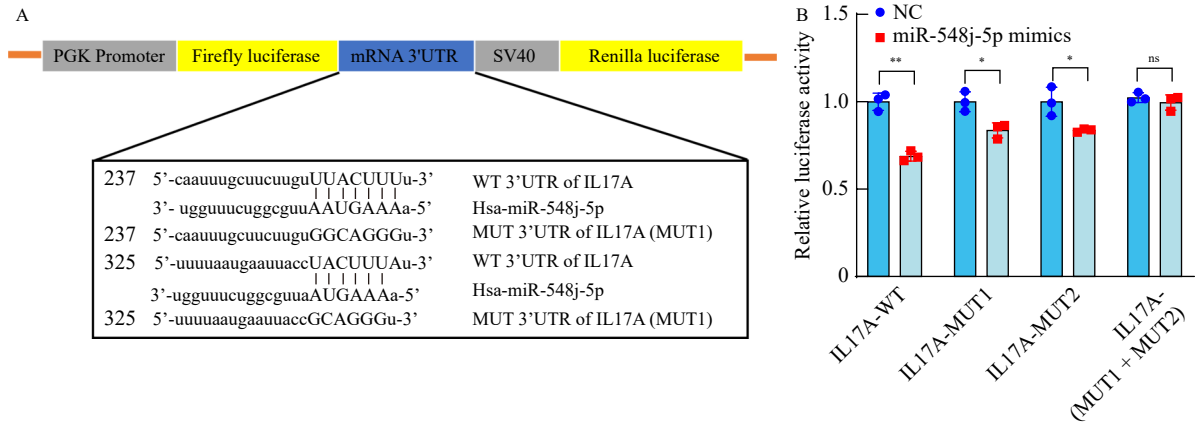

Fig. 5 miR-548j-5p directly targets *IL17A* mRNA 3′UTR. (A) Hypothetical miRNA target site in *IL17A* mRNA 3'UTR, as well as luciferase constructs of wild-type (WT) and mutant (MUT). (B) The luciferase activity is determined by co-transfecting the vectors (*IL17A* 3'UTR-WT and MUT1, MUT2, or MUT1 + MUT 2) combined with NC, miR-548j-5p mimics into 293T cells, respectively. Data are presented as the mean ± SD. $^{*}P < 0.05$, $^{**}P < 0.01$ *vs* NC.

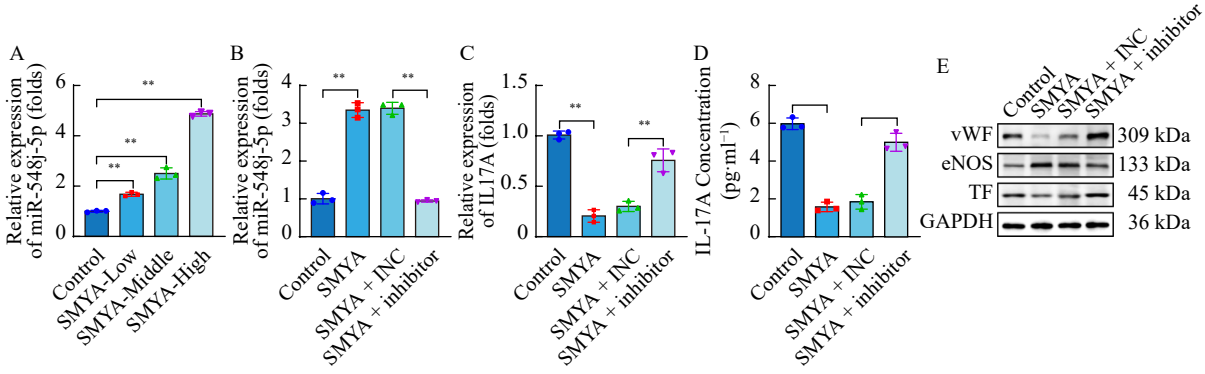

Fig. 6 miR-548j-5p inhibition attenuates the efficacy of SMYA-containing serum *in vitro*. (A) Detection of the expressions of miR-548j-5p dependent on different SMYA doses by qRT-PCR in HUVECs of Control, SMYA-Low group, SMYA-Middle group, and SMYA-High group. (B) The changes of miR-548j-5p levels in HUVECs of Control, SMYA-High, SMYA-High + INC, SMYA-High + inhibitor groups using qRT-PCR. (C, D) Assays of *IL17A* mRNA and IL-17A protein levels by qRT-PCR and ELISA in HUVECs of Control, SMYA-High, SMYA-High + INC, SMYA-High + inhibitor groups. (E) Expressions of vWF, eNOS, and TF protein were determined by Western blotting in HUVECs of Control, SMYA-High, SMYA-High + INC, and SMYA-High + inhibitor groups. Data are presented as the mean ± SD. $^{**}P < 0.01$ *vs* Control.

rently, the protein levels of vWF and TF in the vascular tissue of TAO rats treated with the miR-548j-5p inhibitor were elevated, while the expression of eNOS was decreased (Fig. 7J). These findings suggest that inhibition of miR-548j-5p could exacerbate thrombosis by increasing the expression of IL-17A and lead to vascular endothelial dysfunction.

Discussion

Mounting evidence indicates that inflammation plays a critical role in the complex pathological processes of TAO, including its significant contribution to thrombosis. Plaque rupture, a key event in thrombosis, facilitates the release of inflammatory cytokines [38, 39]. Furthermore, SMYA targets key inflammatory mediators such as IL-17A, interleukin-6 (IL-6), tumor necrosis factor (TNF), and vascular endothelial growth factor (VEGF) to treat vascular diseases [40-42]. Functionally, SMYA reduces the infiltration of inflammatory cells into vascular tissues, protects vascular endothelial cells, stabilizes plaques, inhibits platelet aggregation, and helps prevent thrombosis. However, the precise mechanisms through which SMYA acts on TAO remain largely unclear. Our experimental research has demonstrated that SMYA exerts an inhibitory effect on IL-17A, mediated through the regulation of miR-548j-5p (Fig. 8).

IL-17A is a potent immunomodulatory cytokine that [43], upon secretion, binds to its receptor and promotes the production of inflammatory mediators such as interleukin-6 (IL-6) and interleukin-8 through various signaling pathways [44, 45]. Experimental studies in mice have demonstrated that treatment with an IL-17A antibody leads to decreased cell infiltration, reduced secretion of cytokines and chemokines, and lowered biomarkers for endothelial and immune cell activity [46]. This evidence underscores the significant role of IL-17A in the interplay between inflammation and coagulation reactions. Despite these findings, the specific involvement of IL-17A in the pathogenesis of TAO remains unclear. In our experimental study, we observed a significant upregulation of IL-17A in both TAO patients and TAO model rats. Neutralizing IL-17A activity in TAO rats substantially inhibited thrombus formation, suggesting that elevated IL-17A levels

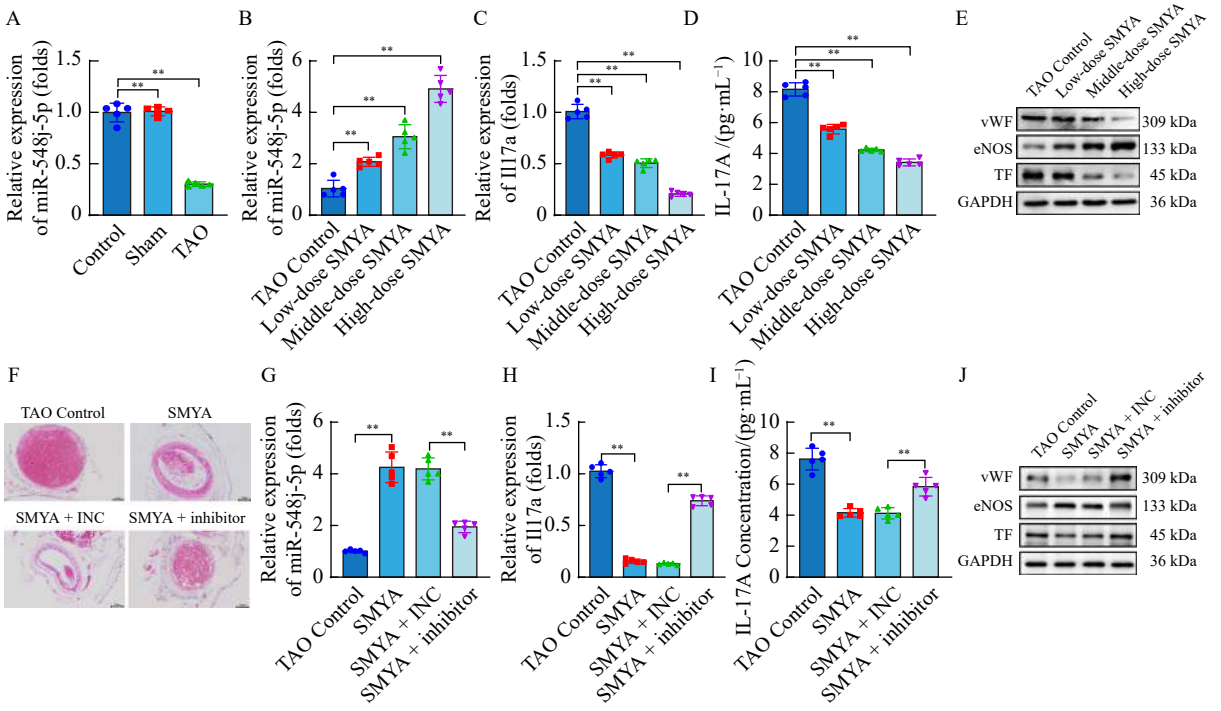

Fig. 7 Inhibition of miR-548j-5p invalidates SMY's therapeutic effect *in vivo*. (A) The expressions of miR-548j-5p were determined by qRT-PCR in the vascular tissue of rats in the Control, Sham, and TAO groups (n = 5). (B) The dependence of SMYA-regulated miR-548j-5p levels in the vascular tissue of rats in the TAO Control, Low-dose SMYA, Middle-dose SMYA, and High-dose SMYA groups (n = 5) by qRT-PCR. (C, D) The determination of *IL-17A* mRNA protein levels by qRT-PCR and ELISA in vascular tissue of TAO Control, Low-dose SMYA, Middle-dose SMYA, High-dose SMYA groups (n = 5). (E) Expression of vWF, eNOS, and TF protein were determined by Western blotting in the vascular tissue of rats in the TAO Control, Low-dose SMYA, Middle-dose SMYA, and High-dose SMYA group (n = 5). (F) H&E staining (magnification, × 100) in the vascular tissue of rats in the TAO Control, High-dose SMYA, High-dose SMYA + INC, and High-dose SMYA + inhibitor groups (n = 5), scale bar = 100 μm. (G, H, I) The floating in miR-548j-5p, *IL-17A* mRNA, and IL-17A protein levels partly determined by qRT-PCR and ELISA in the vascular tissue of rats in the TAO Control, High-dose SMYA, High-dose SMYA + INC, and High-dose SMYA + inhibitor groups (n = 5). (J) The corresponding vWF, eNOS, and TF protein expressions were estimated by Western blotting assay in the vascular tissue of rats in TAO Control, SMYA, High-dose SMYA + INC, High-dose SMYA + inhibitor groups (n = 5). Data are presented as the mean ± SD (n = 5). $^{**}P < 0.01$ *vs* Control; $^{**}P < 0.01$ *vs* TAO Control.

are a potential contributing factor to TAO. Crucially, our findings provide evidence that miR-548j-5p can directly target the 3'UTR of IL-17A, thereby inhibiting its expression. Furthermore, we discovered that a decrease in miR-548j-5p levels leads to increased IL-17A expression and promotes TAO progression. To strengthen the clinical relevance of these findings, it is essential to expand the sample size in future studies to further verify the upregulation of IL-17A during TAO progression.

miRNAs are small, non-coding RNAs that regulate gene expression by binding to the 3'UTR of target mRNAs in a sequence-specific manner. This interaction typically results in the reduction of target gene expression. miRNAs have been demonstrated to play therapeutic roles in various diseases [47-49]. In previous research, specific miRNAs have been shown to inhibit thrombosis by downregulating the expression of pro-inflammatory cytokines such as IL-6 in models of TAO [21, 22]. Furthermore, CHEN *et al.* [50] reported that miR-151 is downregulated in arteriosclerosis obliterans and found that it inhibits endothelial cell apoptosis by targeting IL-17A in this disease context. Despite these findings, the specific role of miRNAs in TAO, particularly regarding the regulation of IL-17A, has not yet been fully elucidated.

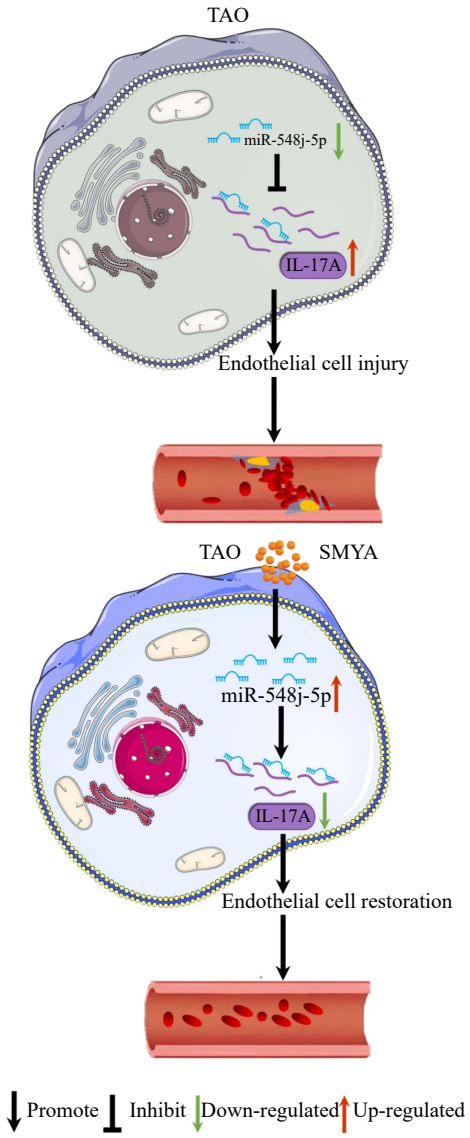

Fig. 8 Schematic diagram of miR-548j-5p/IL-17A signal axis alteration and SMYA intervention mechanism in the pathogenesis of TAO. SMYA can significantly increase the expression level of miR-548j-5p, thereby reducing the level of target gene IL-17A and alleviating the occurrence of TAO. Further elucidating the pathogenesis of TAO from the perspective of epigenetic immune regulation.

miR-548j-5p, a 22-nucleotide long member of the endogenous non-coding single-stranded RNA family, has been shown to promote angiogenesis by stimulating migration and tube formation. It is aberrantly expressed in lung cancer and has been linked to immune responses [51, 52]. In our study, we observed that the downregulation of miR-548j-5p was negatively correlated with the expression of IL-17A. Additionally, *in silico* bioinformatics analysis predicted the presence of complementary binding sites between miR-548j-5p and the IL-17A mRNA 3'UTR. Based on these observations, we hypothesize that the decrease in miR-548j-5p may be a key factor triggering the increase in IL-17A expression in TAO, suggesting a potential therapeutic target in the management of this vascular disease.

Our study revealed that overexpressing miR-548j-5p effectively inhibits IL-17A expression at both mRNA and protein levels. Confirmation of this regulatory interaction was obtained through a dual luciferase reporter assay, which demonstrated direct binding between miR-548j-5p and the IL-17A mRNA 3'UTR. Upon establishing this relationship, we explored the potential of SMYA to modulate the miR-548j-5p/IL-17A axis. We found that SMYA-induced increases in miR-548j-5p expression were inversely correlated with IL-17A levels and contributed to therapeutic effects, including improved vascular endothelium health and reductions in both size and weight of thrombi in rat models. To further validate that SMYA's inhibition of IL-17A is mediated through miR-548j-5p, we employed a mimetic inhibitor to disrupt miR-548j-5p expression. Inhibition of miR-548j-5p markedly diminished the suppressive effects of SMYA on IL-17A gene and protein expression. Consequently, the positive impacts on vascular endothelium and thrombosis were significantly reduced.

In conclusion, our findings indicate that the downregulation of miR-548j-5p enhances IL-17A expression and promotes the development of TAO. Moreover, SMYA mitigates IL-17A expression by upregulating miR-548j-5p. These results underscore the potential of targeting the miR-548j-5p/IL-17A axis as a therapeutic strategy for managing TAO.

References

[1] Zerbino DD, Zimba EA, Bagry NN. Thromboangiitis obliterans (Buerger's disease): state of the art [J]. *Angiol Sosud Khir*, 2016, **22**(4): 185-192.

[2] Rivera-Chavarría IJ, Brenes-Gutiérrez JD. Thromboangiitis obliterans (Buerger's disease) [J]. *Ann Med Surg (Lond)*, 2016, **7**:

79-82.
[3] Cooper LT, Tse TS, Mikhail MA, *et al*. Long-term survival and amputation risk in thromboangiitis obliterans (Buerger's disease) [J]. *J Am Coll Cardiol*, 2004, **44**(12): 2410-2411.
[4] Liu Z, Zhang Y, Zhang R, *et al*. Promotion of classic neutral bile acids synthesis pathway is responsible for cholesterol-lowing effect of Si-miao-yong-an Decoction: application of LC-MS/MS method to determine 6 major bile acids in rat liver and plasma [J]. *J Pharm Biomed Anal*, 2017, **135**: 167-175.
[5] Zhao Y, Sun D, Chen Y, *et al*. Si-Miao-Yong-An Decoction attenuates isoprenaline-induced myocardial fibrosis in AMPK-driven Akt/mTOR and TGF-β/SMAD3 pathways [J]. *Biomed Pharmacother*, 2021, **2021**: 8968464.
[6] Du A, Xie Y, Ouyang H, *et al*. Si-Miao-Yong-An Decoction for diabetic retinopathy: a combined network pharmacological and *in vivo* approach [J]. *Front Pharmacol*, 2021, **12**: 763163.
[7] Chen XN, Ge QH, Zhao YX, *et al*. Effect of Si-Miao-Yong-An Decoction on the differentiation of monocytes, macrophages, and regulatory T cells in ApoE$^{(-/-)}$ mice [J]. *J Ethnopharmacol*, 2021, **276**: 114178.
[8] Qi Z, Li M, Zhu K, *et al*. Si-Miao-Yong-An on promoting the maturation of Vasa Vasorum and stabilizing atherosclerotic plaque in ApoE$^{(-/-)}$ mice: an experimental study [J]. *Biomed Pharmacother*, 2019, **114**: 108785.
[9] Zhu ZB, Song K, Huang WJ, *et al*. Si-Miao-Yong-An (SMYA) Decoction may protect the renal function through regulating the autophagy-mediated degradation of ubiquitinated protein in an atherosclerosis model [J]. *Front Pharmacol*, 2020, **11**: 837.
[10] Zou J, Xu W, Li Z, *et al*. Network pharmacology-based approach to research the effect and mechanism of Si-Miao-Yong-An Decoction against thromboangiitis obliterans [J]. *Ann Med*, 2023, **55**(1): 2218105.
[11] Qiu L, Tan EK, Zeng L. microRNAs and neurodegenerative diseases [J]. *Adv Exp Med Biol*, 2015, **888**: 85-105.
[12] Lozano C, Duroux-Richard I, Firat H, *et al*. MicroRNAs: key regulators to understand osteoclast differentiation? [J]. *Front Immunol*, 2019, **10**: 375.
[13] Tserel L, Runnel T, Kisand K, *et al*. MicroRNA expression profiles of human blood monocyte-derived dendritic cells and macrophages reveal miR-511 as putative positive regulator of Toll-like receptor 4 [J]. *J Biol Chem*, 2011, **286**(30): 26487-26495.
[14] Zhu D, Pan C, Li L, *et al*. MicroRNA-17/20a/106a modulate macrophage inflammatory responses through targeting signal-regulatory protein α [J]. *J Allergy Clin Immunol*, 2013, **132**(2): 426-436.e428.
[15] Wang J, Wang WN, Xu SB, *et al*. MicroRNA-214-3p: a link between autophagy and endothelial cell dysfunction in atherosclerosis [J]. *Acta Physiol (Oxf)*, 2018, **222**(3): e12973.
[16] Li Q, Guo L, Wang J, *et al*. Exosomes derived from Nr-CWS pretreated MSCs facilitate diabetic wound healing by promoting angiogenesis via the circIARS1/miR-4782-5p/VEGFA axis [J]. *Chin J Nat Med*, 2023, **23**(3): 172-184.
[17] Xiao FJ, Zhang D, Wu Y, *et al*. miRNA-17-92 protects endothelial cells from erastin-induced ferroptosis through targeting the A20-ACSL4 axis [J]. *Biochem Biophys Res Commun*, 2019, **515**(3): 448-454.
[18] Song Y, Zhang C, Zhang J, *et al*. Localized injection of miRNA-21-enriched extracellular vesicles effectively restores cardiac function after myocardial infarction [J]. *Theranostics*, 2019, **9**(8): 2346-2360.
[19] Ono K. MicroRNA-133a in the development of arteriosclerosis obliterans [J]. *J Atheroscler Thromb*, 2015, **22**(4): 342-343.
[20] Zhang Y, Zhang Z, Wei R, *et al*. IL (Interleukin)-6 contributes to deep vein thrombosis and is negatively regulated by miR-338-5p [J]. *Arterioscler Thromb Vasc Biol*, 2020, **40**(2): 323-334.
[21] Deng Y, Tong J, Shi W, *et al*. Thromboangiitis obliterans plasma-derived exosomal miR-223-5p inhibits cell viability and promotes cell apoptosis of human vascular smooth muscle cells by targeting VCAM1 [J]. *Ann Med*, 2021, **53**(1): 1129-1141.
[22] Chen B, Deng Y, Wang B, *et al*. Integrated analysis of long non-coding RNA-microRNA-mRNA competing endogenous RNA regulatory networks in thromboangiitis obliterans [J]. *Bioengineered*, 2021, **12**(2): 12023-12037.
[23] von Stebut E, Boehncke WH, Ghoreschi K, *et al*. IL-17A in psoriasis and beyond: cardiovascular and metabolic implications [J]. *Front Immunol*, 2019, **10**: 3096.
[24] Kanaji N, Sato T, Nelson A, *et al*. Inflammatory cytokines regulate endothelial cell survival and tissue repair functions *via* NF-κB signaling [J]. *J Inflamm Res*, 2011, **4**: 127-138.
[25] Shi S, Song L, Liu Y, *et al*. Cotinine aggravates inflammatory response in thromboangiitis obliterans through TLR-4/MyD88/NF-κB inflammatory signaling pathway [J]. *Int Angiol*, 2020, **39**(3): 261-262.
[26] Ding P, Zhang S, Yu M, *et al*. IL-17A promotes the formation of deep vein thrombosis in a mouse model [J]. *Int Immunopharmacol*, 2018, **57**: 132-138.
[27] Dubash S, Bridgewood C, McGonagle D, *et al*. The advent of IL-17A blockade in ankylosing spondylitis: secukinumab, ixekizumab and beyond [J]. *Expert Rev Clin Immunol*, 2019, **15**(2): 123-134.
[28] McGonagle DG, McInnes IB, Kirkham BW, *et al*. The role of IL-17A in axial spondyloarthritis and psoriatic arthritis: recent advances and controversies [J]. *Ann Rheum Dis*, 2019, **78**(9): 1167-1178.
[29] Marder W, Khalatbari S, Myles JD, *et al*. Interleukin 17 as a novel predictor of vascular function in rheumatoid arthritis [J]. *Ann Rheum Dis*, 2011, **70**(9): 1550-1555.
[30] Hot A, Lenief V, Miossec P. Combination of IL-17 and TNFα induces a pro-inflammatory, pro-coagulant and pro-thrombotic phenotype in human endothelial cells [J]. *Ann Rheum Dis*, 2012, **71**(5): 768-776.
[31] Dong M, Tian Z, Ma Y, *et al*. Rapid screening and characterization of glucosinolates in 25 Brassicaceae tissues by UHPLC-Q-exactive orbitrap-MS [J]. *Food Chem*, 2021, **365**: 130493.
[32] Shionoya S. Diagnostic criteria of Buerger's disease [J]. *Int J Cardiol*, 1998, **66 Suppl 1**: S243-245; discussion S247.
[33] Zhao Y, Sun D, Chen Y, *et al*. Si-Miao-Yong-An Decoction attenuates isoprenaline-induced myocardial fibrosis in AMPK-driven Akt/mTOR and TGF-β/SMAD3 pathways [J]. *Biomed Pharmacother*, 2020, **130**: 110522.
[34] Zhang Z, Ji J, Zhang D, *et al*. Protective effects and potential mechanism of salvianolic acid B on sodium laurate-induced thromboangiitis obliterans in rats [J]. *Phytomedicine*, 2020, **66**: 153110.
[35] Park CH, Lee AR, Ahn SB, *et al*. Role of innate lymphoid cells in chronic colitis during anti-IL-17A therapy [J]. *Sci Rep*, 2020, **10**(1): 297.
[36] Jorns A, Ishikawa D, Teraoku H, *et al*. Remission of autoimmune diabetes by anti-TCR combination therapies with anti-IL-17A or/and anti-IL-6 in the IDDM rat model of type 1 diabetes [J]. *BMC Med*, 2020, **18**(1): 33.
[37] Liu C, Kong X, Wu X, *et al*. Alleviation of a disintegrin and metalloprotease 10 (ADAM10) on thromboangiitis obliterans involves the HMGB1/RAGE/ NF-κB pathway [J]. *Biochem Biophys Res Commun*, 2018, **505**(1): 282-289.
[38] Ehteshamfar SM, Afshari JT, Modaghegh MS, *et al*. Humoral and cellular immune response to Buerger's disease [J]. *Vascular*, 2020, **28**(4): 457-464.
[39] Li M, Qi Z, Zhang J, *et al*. Effect and mechanism of Si-Miao-Yong-An on vasa vasorum remodeling in ApoE$^{(-/-)}$ mice with atherosclerosis vulnerable plague [J]. *Front Pharmacol*, 2021, **12**: 634611.

[40] Kaštelan S, Orešković I, Biščan F, *et al*. Inflammatory and angiogenic biomarkers in diabetic retinopathy [J]. *Biochem Med (Zagreb)*, 2020, **30**(3): 030502.
[41] Zhang C, Liu J, Wang J, *et al*. The interplay between tumor suppressor p53 and hypoxia signaling pathways in cancer [J]. *Front Cell Dev Biol*, 2021, **9**: 648808.
[42] Zhou W, Yang L, Nie L, *et al*. Unraveling the molecular mechanisms between inflammation and tumor angiogenesis [J]. *Am J Cancer Res*, 2021, **11**(2): 301-317.
[43] Nordlohne J, von Vietinghoff S. Interleukin 17A in atherosclerosis-regulation and pathophysiologic effector function [J]. *Cytokine*, 2019, **122**: 154089.
[44] Raucci F, Mansour AA, Casillo GM, *et al*. Interleukin-17A (IL-17A), a key molecule of innate and adaptive immunity, and its potential involvement in COVID-19-related thrombotic and vascular mechanisms [J]. *Autoimmun Rev*, 2020, **19**(7): 102572.
[45] Jovanovic DV, Di Battista JA, Martel-Pelletier J, *et al*. IL-17 stimulates the production and expression of proinflammatory cytokines, IL-beta and TNF-alpha, by human macrophages [J]. *J Immunol*, 1998, **160**(7): 3513-3521.
[46] Erbel C, Chen L, Bea F, *et al*. Inhibition of IL-17A attenuates atherosclerotic lesion development in apoE-deficient mice [J]. *J Immunol*, 2009, **183**(12): 8167-8175.
[47] Zhang Y, Miao X, Zhang Z, *et al*. miR-374b-5p is increased in deep vein thrombosis and negatively targets IL-10 [J]. *J Mol Cell Cardiol*, 2020, **144**: 97-108.
[48] Zhang J, Wang C, Guo Z, *et al*. miR-223 improves intestinal inflammation through inhibiting the IL-6/STAT3 signaling pathway in dextran sodium sulfate-induced experimental colitis [J]. *Immun Inflamm Dis*, 2021, **9**(1): 319-327.
[49] Xu H, Cui Y, Liu X, *et al*. miR-1290 promotes IL-8-mediated vascular endothelial cell adhesion by targeting GSK-3β [J]. *Mol Biol Rep*, 2022, **49**(3): 1871-1882.
[50] Chen F, Ye X, Jiang H, *et al*. MicroRNA-151 attenuates apoptosis of endothelial cells induced by oxidized low-density lipoprotein by targeting interleukin-17A (IL-17A) [J]. *J Cardiovasc Transl Res*, 2021, **14**(3): 400-408.
[51] Lee CY, Lin SJ, Wu TC. miR-548j-5p regulates angiogenesis in peripheral artery disease [J]. *Sci Rep*, 2022, **12**(1): 838.
[52] Halvorsen AR, Sandhu V, Sprauten M, *et al*. Circulating microRNAs associated with prolonged overall survival in lung cancer patients treated with nivolumab [J]. *Acta Oncol*, 2018, **57**(9): 1225-1231.

Cite this article as: CHU Chu, SUN Shangwen, ZHANG Zhen, *et al*. Si-Miao-Yong-An Decoction alleviates thromboangiitis obliterans by regulating miR-548j-5p/IL-17A signaling pathway [J]. *Chin J Nat Med*, 2024, **22**(6): 541-553.